Helmholtz-Zentrum Dresden-Rossendorf (HZDR)

Influence of MIBC on the surface-air nucleation and bubble-particle loading in graphite froth flotation

Xu, M.; Vanderbruggen, A.; Kupka, N.; Zhang, H.; Rudolph, M.;

Perma-Link to Publication Repository of HZDR:

https://www.hzdr.de/publications/Publ-36134

Influence of MIBC on the surface-air nucleation and bubble-particle loading in graphite froth flotation

Ming Xu[a], Anna Vanderbruggen[a], Nathalie Kupka[b], Haijun Zhang[c], Martin Rudolph[a]

a. Helmholtz-Zentrum Dresden-Rossendorf, Helmholtz Institute Freiberg for Resource Technology, Freiberg 09599, Germany

b. Metso:Outotec Oyj, Espoo 002230, Finland

c. School of Chemical Engineering and Technology, China University of Mining & Technology, Xuzhou, Jiangsu 221116, China

Abstract:

This paper investigates one aspect of surface air nucleation in froth flotation, namely the impact of frother-type surfactants like Methyl isobutyl carbinol (MIBC). During this study, tap water was pressurized in an autoclave to produce air-oversaturated water for air nucleation precondition in flotation. Various experiments were carried out with graphite particles to investigate the influences of gas nucleation and MIBC on flotation: micro-flotation, single bubble collision experiments in hydrodynamic conditions and pick-up experiments in static conditions. In addition, microscopic observations were combined with agglomeration analysis to clarify the effects of the frother MIBC on the air nucleation and agglomerate formation. The experimental results show the combination of MIBC and air nucleation can significantly increase the graphite recovery compared to using air-oversaturated water or normal tap water with MIBC alone, respectively. The analysis indicates that MIBC can improve the air nucleation probability on graphite surfaces by enhancing the stability of the air nuclei to form more microbubbles on the surface. Meanwhile, the surface microbubbles can collide with other particles forming coarser aggregates, improving their collision probability and with this increasing the recovery of fine particles. Furthermore, the results show that MIBC can reduce the detachment of particles from the surface of nucleation

bubbles, leading to an increase in particle load of the bubble-particle aggregates in hydrodynamic conditions, improving the graphite recovery significantly.

Keywords: graphite, air nucleation, agglomeration, frother

1. Introduction

Froth flotation is a well-established process to separate target/valuable minerals from gangue (Wills and Finch, 2015). In the flotation process, the dissolved gas molecules in gas oversaturated water can diffuse into the nucleated sites such as the crevices and holes on the mineral surfaces to form surface microbubbles or nanobubbles (Pradhan et al., 2019). Surface micro-bubbles or nanobubbles on mineral surfaces can act as a secondary collector to enhance the attachment process to improve the recovery of minerals, sparking the interest of many researchers (Sabereh et al., 2019; Pradhan et al., 2019; Zhang et al., 2012). When the solid samples are immersed in water, the water cannot exclude all the gas from the crevices and holes on the sample surfaces, especially for hydrophobic surfaces. These remaining gas reservoirs on the surface were defined as the entrainment gas. A considerable amount of literature has shown that the entrainment gas in the crevices, pores, and valleys on the solid surfaces can significantly reduce the nucleation energy barrier (Aquilano et al., 2003; Yuan et al., 2016). The stability of this entrainment gas can be enhanced by the adsorption of surfactants in the gas-liquid interface (Jones et al., 1999; Satpute and Earthman, 2021).

Surfactant molecules, can adsorb in the gas-liquid surface to form a stable water film, improving the gas nuclei stability on mineral surfaces, leading to an improvement of gas nucleation probability on mineral surfaces (Yount et al., 1984). Edvard A. Hemmingsen found surfactants can significantly reduce the gas nucleation thresholds when the molecular weights of the surfactants are below 330 Da (Hemmingsen, 1978). Tanaka et al. found surfactants can weaken the driving force of mass transfer and slow down the dissolution speed of microbubbles (Alves et al., 2005; Tanaka et al., 2020). Apart from the surfactant effects on the size and stability of external bubbles, it should be highlighted that surfactants can also enhance the stability of surface gas nuclei when

flotation is carried out in gas oversaturated water. Indeed, surfactants in gas-oversaturated water can increase the nucleation probability, leading to more surface microbubbles forming on the mineral surfaces and improving the flotation recovery.

Typically the flotation process is divided into three sub-processes: collision, attachment, and detachment of (mineral) particles to external carrying bubbles. Flotation reagents play essential roles to enhance attachment and weaken detachment processes. One group of such reagents are referred to as frother-type surfactants mostly used to promote flotation efficiency by adsorbing in the gas-liquid interface to reduce surface tension, inhibit bubble coalescence, improve bubble stability, enabling smaller bubbles, and promoting foam stability (Le et al., 2012; Liu et al., 2020; Liu et al., 2021; Nuorivaara and Serna-Guerrero, 2020; Parhizkar et al., 2015). Xu et al. (2019) used a nonionic surfactant TX-100 (4-Octylphenol polyethoxylated) to reduce the size of carrying bubbles and improve the stability of bubbles and foams in flotation, which can significantly improve the recovery of fine unburned carbon particles from fly ash. Xiao et al. (2019) found that sodium oleate can significantly increase the concentration of nanobubbles in solution, improving the recovery of fine-grained minerals. Some surfactants can also adsorb on mineral surfaces to modify wettability, thereby influencing the flotation result (Chen et al., 2021; Liu et al., 2019; Peng et al., 2019; Ruan et al., 2021; Zhao et al., 2021). As the hydrophobicity increases, more gas nuclei will be entrapped on mineral surfaces, and the gas nucleation probability will increase (Jones et al., 1999). Some studies have investigated the influences of the adsorption of MIBC on the wettability of coal surfaces which contain oxygen functional groups, aromatic groups, and hydrocarbon groups (Cao, L., et al., 2021; Ozmak, M & Aktas, Z., 2006). The hydroxyl group of MIBC could interact with oxygen functional groups on the coal surfaces to form hydrogen bonds to improve the hydrophobicity of coal surfaces. The aliphatic hydrocarbon groups of MIBC and coal could interact with each other to form the weak CH/π interaction which is unable to change the surface hydrophobicity of coal. However, the graphite surfaces just have the carbon atoms which could interact with the aliphatic hydrocarbon groups of MIBC and the hydroxyl groups are toward to water phase which has little influences on the wettability of the surfaces.

Recently, the reuse of fine-grained minerals and tailings has attracted the considerable attention of many researchers. However, the particle size of the liberated products of these minerals and tailings is very fine to ultra fine, which causes many problems in minerals flotation. Fine particles are difficult to float due to the low probability of collision and attachment to coarser carrying bubbles. Moreover, the high relative surface areas of fine particles can increase the consumption of reagents (Miettinen et al., 2010). To improve the recovery of fine particles, many methods such as reducing carrying bubbles size with frothers or the use of macromolecule polymers for agglomeration flotation have been developed. The formation of surface nanobubbles and microbubbles due to gas nucleation can improve flotation efficiency in several aspects: selective formation on hydrophobic mineral surfaces or enhancing the attachment to carrying bubbles by gas capillary bridging (Farrokhpay et al., 2020, Shahbazi et al., 2010). These advantages of surface nanobubbles and microbubbles can reduce the flotation reagent consumption by acting as a secondary collector.

During flotation, the fluid can induce the wave of bubble surfaces to force the particles to detach from its carrying bubble. The nucleation microbubbles can collide with particles, forming aggregates to enhance flotation efficiency which can be seen as a secondary agglomeration flotation effect. The surfactant can improve the stability of the nucleation microbubbles, preventing the coalescence of the aggregates generated by nucleation bubbles and reducing the wave of the microbubble surfaces to avoid the particle detachment from the aggregates, and with this improve the particle load of the aggregates (Aoki et al., 2015a; Aoki et al., 2015b; Bournival et al., 2014; Bournival et al., 2015; Bournival et al., 2012). The tiny surface microbubbles at the early nucleation stage can improve the attachment probability to the fine particles. Furthermore, as the load of nucleation bubbles increases, the sizes of the aggregates are also increased, which can promote the collision probability to carrying bubbles, and then improve the minerals recovery, especially for fine particles (Chipfunhu et al., 2011; Miettinen et al., 2010; Rulyov et al., 2021).

In the case of hydrophobic minerals with rough surfaces, the degree of gas oversaturation in water required for gas nucleation is low. Many devices such as micro-bubble generators or pumps can

suck and pressurize air into water to generate gas-oversaturated water in flotation plants even if it was not the main purpose of such machinery. The possible influences of air nucleation on minerals flotation have been discussed in our previous work (Xu et al., 2022). The promotion effects of air-oversaturated water on the recovery of graphite in flotation without regeants were proved by the capillary bridging effect of surface microbubbles and the formation of bubble-partcile agglomerations. Meanwhile, the selectivity of the air nucleation on graphite surfaces compared to quartz surfaces was also certified. Therefore, it is necessary to investigate the influences of gas nucleation and surfactants on flotation performances as such effects could be employed to significantly improve the overall recovery of valuables.

This study aims to clarify the role of frother-type surfactants on gas nucleation and graphite flotation performances with air-oversaturated water. The main effects are explained from two perspectives: one is the formation probability of the nucleation bubbles on the mineral surfaces; the other is the load of carrying bubbles and aggregates formed by the collision of gas nucleation microbubbles and graphite particles.

2. Materials and methods.

2.1. Materials

The surfactant, Methyl isobutyl carbinol (MIBC), supplied by Alfa Aesar (99 % $C_6H_{14}O$, Product No. A13435), was chosen for this study as it is widely used in flotation plants. Moreover, MIBC can improve the stability of bubbles and has little effect on the wettability of graphite surfaces (Miller et al., 1983). A high concentration MIBC solution (2×10^{-2} mol/L) was prepared using deionized water (Helmholtz Institute, Freiberg, Germany) for dilution to get low concentration (1.5×10^{-5} mol/L). The average size of the graphite used in the flotation experiments was 22 μm. The tap-density of the graphite is about 0.97 g/cm^3 and the theoretical density of graphite is 2.26 g/cm^3. A 20 μm sieve was used to separate the graphite, and then the + 20 μm fraction was used for agglomeration experiments (the gas nucleation probability is high on coarser particle surfaces because of more crevices and holes on the surfaces). The graphite sample was purchased

from ProGraphite GmbH with 99.99 % carbon content. In order to observe more nucleation bubbles, the size of the graphite particles for gas nucleation probability statistic was in the range of 50-80 μm, which was produced by crushing a bulk graphite purchased from ward's science company. The tap water (Helmholtz Institute, Freiberg, Germany) was sealed in an autoclave under 3 bar air pressure (overpressure) for 4 hours to obtain the air-oversaturated water. The degree of gas saturation increases with conditioning pressure according to Henry's law, i.e. the amount of dissolved gas in a liquid is proportional to its partial pressure above the liquid, and the proportionality factor is known as it's Henry's constant. The contact angle of a highly oriented pyrolytic graphite (HOPG, μmasch, ZYB, $77.4 \pm 0.85°$) was used to represent the contact angle of the graphite particles.

2.2. Micro-flotation experiments

A series of micro-flotation experiments were carried out in a Hallimond tube, which was designed at the TU Bergakademie Freiberg with gas sparging through a frit to study the graphite flotation performances. The micro-flotation experiments were carried out at 20°C ($\pm$ 0.5°C) with 1 g pure graphite in different waters (tap water and air-oversaturated water) with and without MIBC. The pH of the flotation solution was 7. The dosage of the MIBC is 1.5×10^{-5} mol/L, and no other reagent was added in the micro-flotation experiments. The flotation pulp with a volume of 160 mL was agitated in a beaker for 120 s with and without MIBC. After the agitation, the pulp was transferred to the Hallimond tube. The Hallimond tube is equipped with a magnetic stirrer rotating at 500 rpm to further disperse the particles for another 480 s. After the conditioning, the airflow was set to 20 cm^3/min for collecting concentrates and the collecting times were 10 s and 240 s. After flotation, the concentrates and tailings were collected separately on filters using a vacuum filter and dried at 50°C - 60°C in a drying oven until mass constancy was reached. The resulting mass balance was checked for losses, and tests with losses above 10 % were rejected. The recoveries of the tailings and concentrates were calculated based on the tailing and concentrate masses.

2.3. Single bubble collision and pick-up experiments

An optical contour analysis instrument (OCA 50 Pro, DataPhysics, Germany) was used for the single bubble collision and pick-up experiments (Chu et al., 2014; Nowak and Pacek, 2015; Verrelli and Albijanic, 2015) to figure out the influences of dissolved air and MIBC on the attachment and detachment processes of graphite particles to carrying bubbles in flotation. The experiments were performed at 20°C (± 0.5°C).

The single bubble collision experiments in hydrodynamic conditions were used to analyze the combined influences of attachment and detachment processes in flotation, as shown in Fig.1. The procedure is as follows: (i) a 0.5 g graphite sample was conditioned in 80 mL different waters (tap water and air-oversaturated water) with and without MIBC (1.5×10^{-5} mol/L) using a magnetic stirrer at 500 rpm for 480 s. (ii) After most of the particles settled to the bottom of the cuvette and the supernatant clarified, the cuvette was placed on the table of the OCA 50, and (iii) an 80 μL gas bubble was generated by a needle with 1.37 mm inner diameter connected to a glass syringe in the solution. The variations of diameters of pick-up bubbles are smaller than 5 %. Following the generation of the bubble, (iv) the magnetic stirrer was turned on at 300 rpm (the solution is translucent with the background light and it can be seen that all the paticles are well suspended during the agitation) to disperse the graphite particles for 10 s. The position of the needle is fixed and the position of the cuvette is marked on the objective table of the OCA device to ensure the bubble is on the same position in each experiment. During the agitation, the graphite particles can collide and attach to the bubble depending on the likelihood of those subprocesses. (v) After the supernatant clarified, the images of the bubbles were saved and the coverage angles of graphite particles on the bubble θ were determined. After the measurement, (i), (ii), (iii), (iv), (v) were repeated in the following experiment. Each condition was repeated five times.
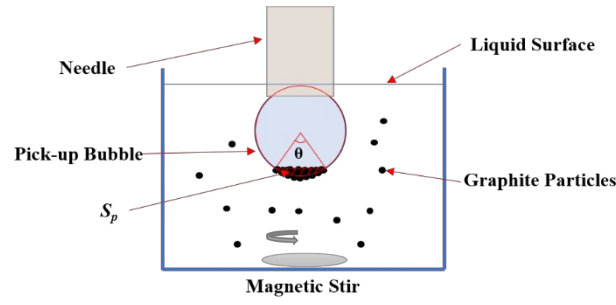
Fig. 1. Single bubble collision experiments in hydrodynamic condition

The single bubble pick-up experiments in static conditions were used to investigate the effect of MIBC on the attachment process of graphite particles to the carrying bubble in normal water. The procedure is shown in Fig. 2. First, a 2 g graphite sample was conditioned in an 80 mL cuvette in tap waters with and without MIBC (1.5×10^{-5} mol/L) using a magnetic stirrer at 800 rpm for 480 s, and the magnetic stirrer was taken out immediately after agitation. After most of the particles settled to the bottom of the cuvette and the supernatant clarified, the cuvette was placed on the table of the OCA, and an 80 μL gas bubble was generated by a needle with 1.37 mm inner diameter connected to a glass syringe in the solution. The variations of diameters of pick-up bubbles are smaller than 5 %. Following its generation, the bubble was moved down slowly to press in the graphite particle bed and kept there for 10 s. For each experiment, the lower end of the needle is set to the same horizontal position to control the bubble-particle bed pressing and bubble deformation to be constant. Then, the bubble was moved upwards for imaging, and the tests were repeated five times at different positions of the particle bed for each condition.
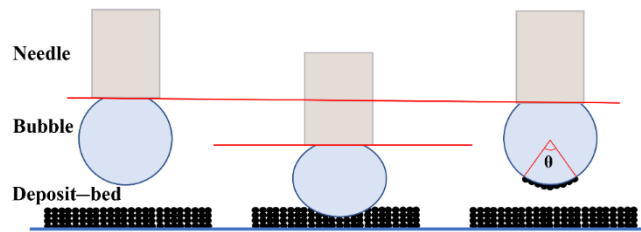

Fig. 2. Single bubble pick-up experiments in static condition

2.4. Agglomeration experiments with laser diffraction

The size distribution of graphite (partially agglomerated) in the solution was analyzed by a laser

diffraction device equipped with a cuvette (HELOS, Sympatec, Germany) to investigate the influence of MIBC on the (fine) graphite particle agglomeration performance in the air-oversaturated water. The schematic diagram of the device is shown in Fig.3. It was used to investigate the agglomeration behaviors in air-oversaturated water with and without MIBC. The experiments were conducted at about 20°C (± 0.5°C). The graphite particles were dispersed by a magnetic stirrer at 2500 rpm within the cuvette. In each measurement, the background in pure air-oversaturated water was substracted. The cuvette was cleaned and hydrophilized by oxygen plasma to avoid nucleation bubbles on the glass surface, so there are little nucleation bubbles in the pure air-oversaturated water. A 30 mg sample was dispersed in 30 mL different waters (normal tap water and gas over-saturated water) with and without MIBC. In order to extend the difference with the small particles concentration, the + 20 μm fraction of the particles was used for the experiments. To avoid the bubble and floc attachment on the cuvette wall, the cuvette was cleaned and treated with oxygen gas plasma for 300 s before each experiment to render the cuvette wall properly water wettable avoiding gas nucleation on the cuvette walls. The measuring range of the optical lens in the tests is 0-875 μm. 60 s after adding the particles, the size distributions were measured.

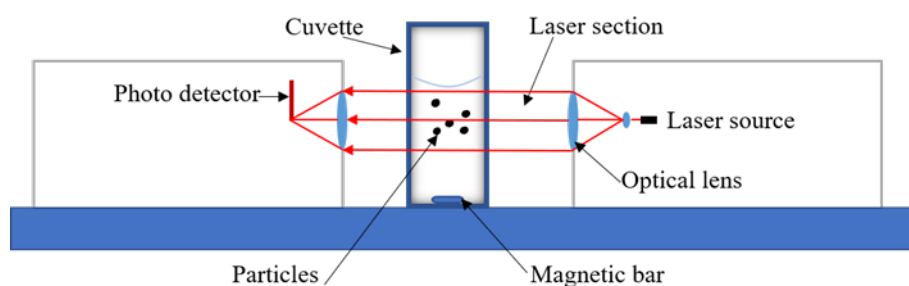

Fig. 3. The sketch of the laser diffraction device

2.5. Microscopic analysis

A microscope equipped with a special transparent cuvette was used to observe the influence of MIBC on the air nucleation process of surface microbubbles in air-oversaturated water. Before each experiment, the cuvette was cleaned with deionized water, isopropanol, ultrasound, and

processed in the oxygen gas plasma for 300 s to reduce bubble nucleation on the cuvette wall. The experiments were executed at about 20°C (± 0.5°C). Firstly, air-oversaturated waters with and without MIBC were prepared and the procedures are as follows: 30 µL high concentration MIBC solution (2×10^{-2} mol/L) was added in 40 mL air-oversaturated water and the solution was agitated by a magnetic stirrer (200 rpm) for 30 s to get the air-saturated water with MIBC (1.5×10^{-5} mol/L); similarly, for air-saturated water without MIBC, 30 µL normal deionzed water was added into 40 mL air-oversaturated water and the solution was agitated by the magnetic stirrer (200 r/min) for 30 s. After the water preparation, 20 mg particles were weighted for each experiment and dispersed in the solution by the magnetic stirrer (200 rpm) for 60 s. After the particles settled to the bottom of the beaker, a pipette was used to sample the deposited particles and transfer them to the cuvette. The cuvette was then placed on the objective table to observe surface micro-bubbles; fourteen experiments were done in repeat. The samples were observed under 2.5 x and 10 x magnification. The air-oversaturated degree has significant influence on the air nucleation probabilities. After the release of the pressure of the autoclave, the air-oversaturated degree will gradually decrease as time goes on, so the overall time of the procedure of each experiment was controlled to be the same to ensure the same degree of air-ovesaturation for the start of air nucleation processes.

3. Results

3.1. Micro-flotation experiments

Fig. 4 illustrates the micro-flotation recoveries of the graphite in different waters with and without MIBC when the collecting time is 240 s. This figure shows that the average recovery of graphite flotation without MIBC increased from 30.40 ± 0.75 % in tap water to about 34.71 ± 1.21 % in air-oversaturated water. After the addition of MIBC, the average recovery increased from about 39.95 ± 1.29 % in tap water to about 55.86 ± 1.78 % in air-oversaturated water. The recovery increases significantly after the addition of MIBC regardless of the type of water. Meanwhile, the increased recovery in air-oversaturated water (21.15 %) is more than double the one in tap water (9.55 %). During the conditioning process in air-oversaturated water, many aggregates formed due

to the collision of gas nucleation bubbles and the graphite particles. These aggregates floated and attached to the wall of the Hallimond tube, as shown in Fig. 5. Most of the particles in the concentrate came from the aggregates on the Hallimond tube wall when the collecting time of concentrates is 10 s. The average recovery in this case increased from 5 % in flotation without MIBC to 21 % in flotation with MIBC, which can be well explained by more aggregates formed in flotation with MIBC.
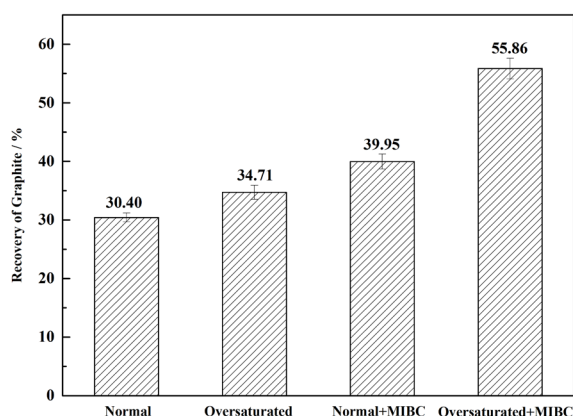

Fig. 4. Graphite recoveries with different conditions: water type and MIBC reagent, the error bars represent the 95% confidence intervals

Fig. 5. The formation of aggregates during the conditioning process

3.2. Single bubble collision and pick-up experiment

The average coverage angles in different waters in single bubble collision experiments are shown in Fig. 6.
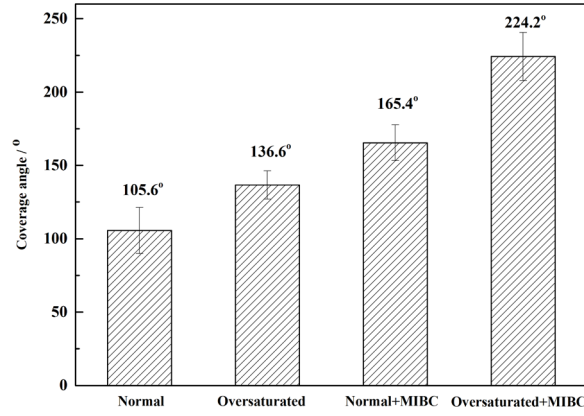
Fig. 6. The coverage angle in hydrodynamic condition with different waters the error bars represent the 95% confidence intervals

The coverage percentages of particles are calculated by equation (1) which can be used to compare the differences of particles-loading behaviours of the carrying bubbles in different waters

$$P_a = \frac{S_1}{S} \times 100\% \quad (1)$$

Where S_1 is surface areas covered by particles on the carrying bubble and S is the whole surface area of the carrying bubble. All the carrying bubbles are assumed to be sphere. The coverage percentages of P_a can be obtained through the particles coverage angle θ. The derived processes are shown in equation (2) (3) (4).

$$S_1 = 2\pi r^2 \left(1 - cos\frac{\theta}{2}\right) \quad (2)$$

$$S = 4\pi r^2 \quad (3)$$

$$P_a = \frac{1 - cos\frac{\theta}{2}}{2} \times 100\% \quad (4)$$

Where r is the radius of the carrying bubble. The representative pictures of single bubble collision experiments under the hydrodynamic condition are shown in Fig. 7. In collision experiments without MIBC, the average coverage angle increased from $105.6º \pm 15.7º$ in tap water to $136.6º \pm 9.7º$ in air-oversaturated water. The coverage areas percentages increased from $20.0\% \pm 5.7\%$ in tap water to $31.6\% \pm 3.9\%$ in air-oversaturated water. In collision experiments with MIBC, the average coverage angle increased from $165.4º \pm 12.2º$ in tap water to $224.2º \pm 16.3º$ in air-oversaturated water. coverage areas percentages increased from $43.7\% \pm 5.3\%$ in tap water to $68.7\% \pm 6.6\%$ in air-oversaturated water.

In the particles collision experiments under the same hydrodynamic condition, the differences of coverage angles are determined by both attachment and detachment. The shear flow in the cuvette can induce the shaking off of the bubble and the fluctuation of the bubble surface which can induce the relative move of the particles to the bubble surface and enforce the detachment of the particles from the bubble surface (Nguyen and Evans, 2004; Wang et al., 2003).

The representative pictures in single bubble pick-up experiments under the static condition were shown in Fig. 8. The average coverage angles decreased from $99.9^o \pm 1.55^o$ in tap water without MIBC to $93.8^o \pm 2.16^o$ in tap water with MIBC, which means that MIBC can weaken the attachment process of the particles to the pick-up bubble. The pick-up experiments are mainly influenced by the attachment process. During the attachment process, the rupture of the hydration film on the bubble surface with MIBC is more difficult when the pick-up bubble was pressed onto the partciles because the polar group of MIBC pointed towards water phase can strengthen the hydration film compared to the bubble without MIBC (Arturo et al., 2015; Ralston et al., 1995).

It can be found significant higher covarge angles in normal tap water with MIBC compared to without MIBC in particles collision experiments, and the little difference of coverage angles in normal tap water with MIBC compared to without MIBC in pick-up experiments which means MIBC has little influences on the attachment process, so the significant differences of the coverage angles in the particles collision experiments should be caused by the detachment process. Thus, it can be concluded that MIBC most likely reduces the detachment probability of the particles from the bubble in the hydrodynamic condition of the single bubble collision experiments which includes both effects of attachment and detachment.
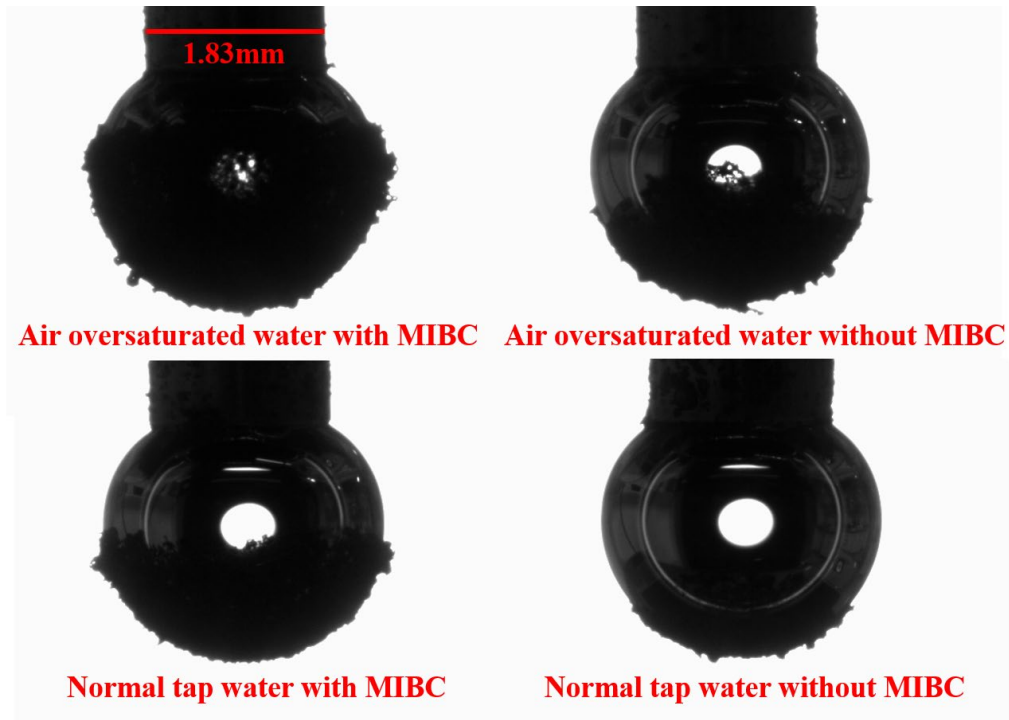
Fig. 7. The represent pictures in hydrodynamic condition with different waters

Fig. 8 The represent pictures in static condition in the tap water with and without MIBC

3.3. Microscopic observations

Fig. 9 shows two bubble nucleation events at a crevice and a hole on the graphite surface in air-oversaturated water.
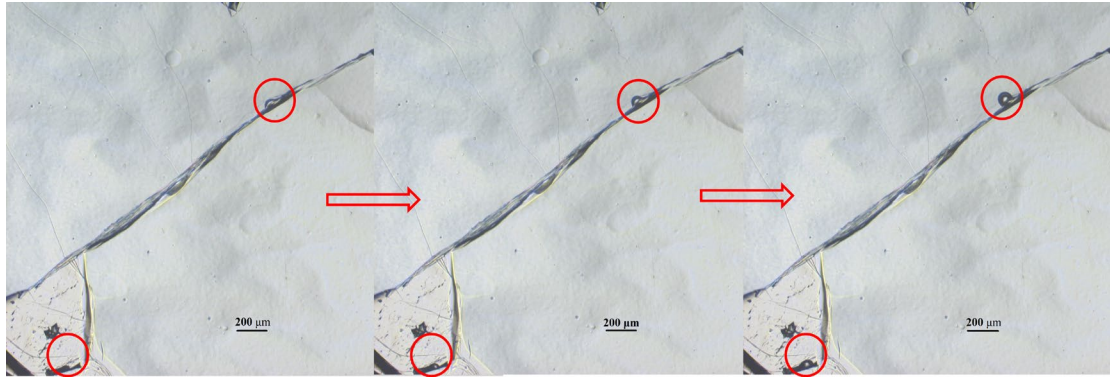
Fig. 9. Gas nucleation from the crevice and hole on the graphite surface

Many aggregates formed and floated during the conditioning process of flotation in air-oversaturated water with and without MIBC. A pipette was used to sample these aggregates and transfer them into a cuvette for observation with a microscope. The structure of the aggregates is shown in Fig. 10. The aggregates are composed of nucleation bubbles and graphite particles. Fig. 11 and Fig. 12 shows the bubble nucleation process in 2 minutes on the surface of graphite particles in air-oversaturated water with and without MIBC, respectively. The left and right pictures were taken at beginning and after 2 min. The alteration of the highlighted particles is caused by the growth of surface microbubbles. The nucleation probability was calculated using the formula (5)

$P=N_n/N_o$ (5)

Where N_n is the number of the particles with surface nucleation microbubble(s) (as observable with the method); N_o is the overall number of the particles. From the statistic of 14 pictures of each condition, 531 and 518 particles were counted in air-oversaturated waters with and without MIBC respectively. The nucleation probabilities with MIBC and without MIBC were 9.6 % and 5.2 % respectively and the confidence level of the different nucleation probability is 0.99. It can be found that MIBC can improve the gas nucleation probability on the graphite surfaces in air-oversaturated water.
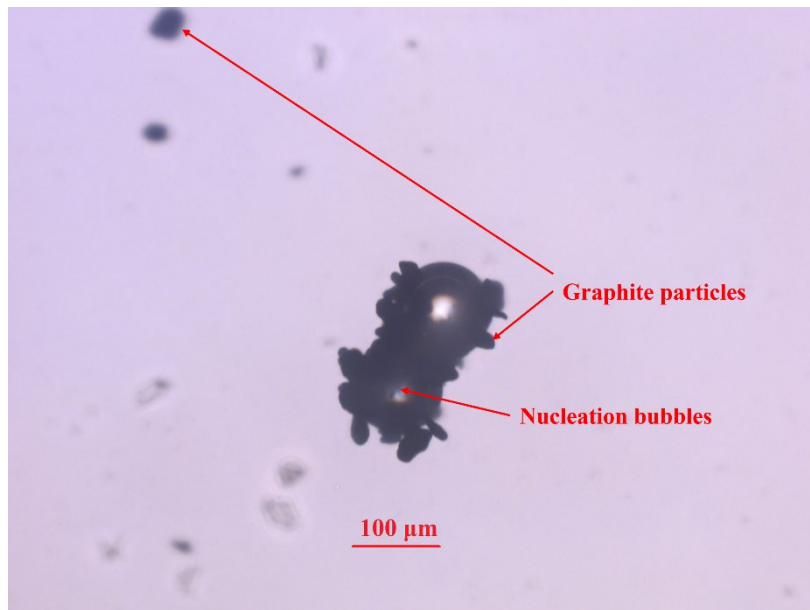
Fig. 10. The structure of a floc in oversaturated water under the microscope
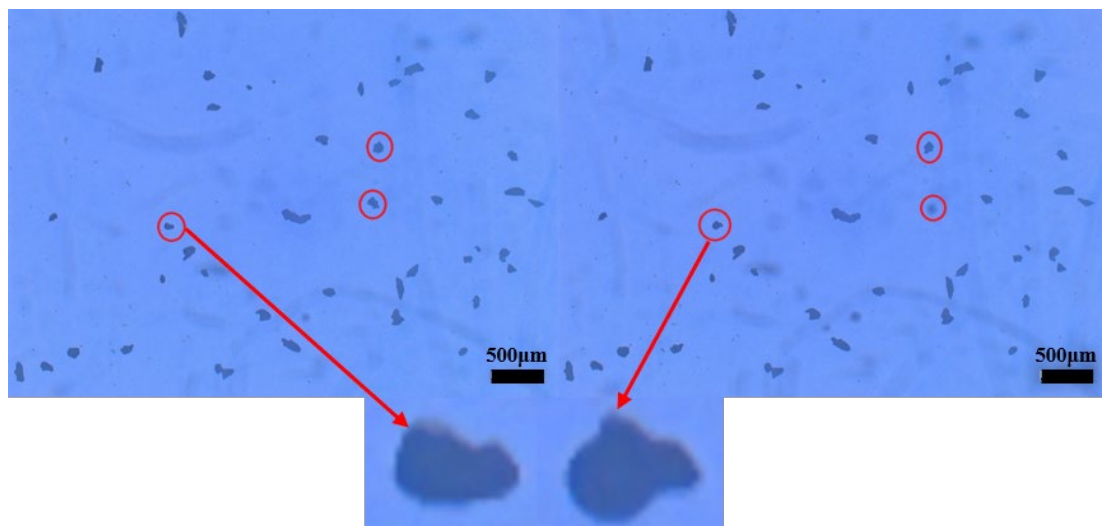

Fig. 11. Gas nucleation on graphite particle surfaces in oversaturated water with MIBC
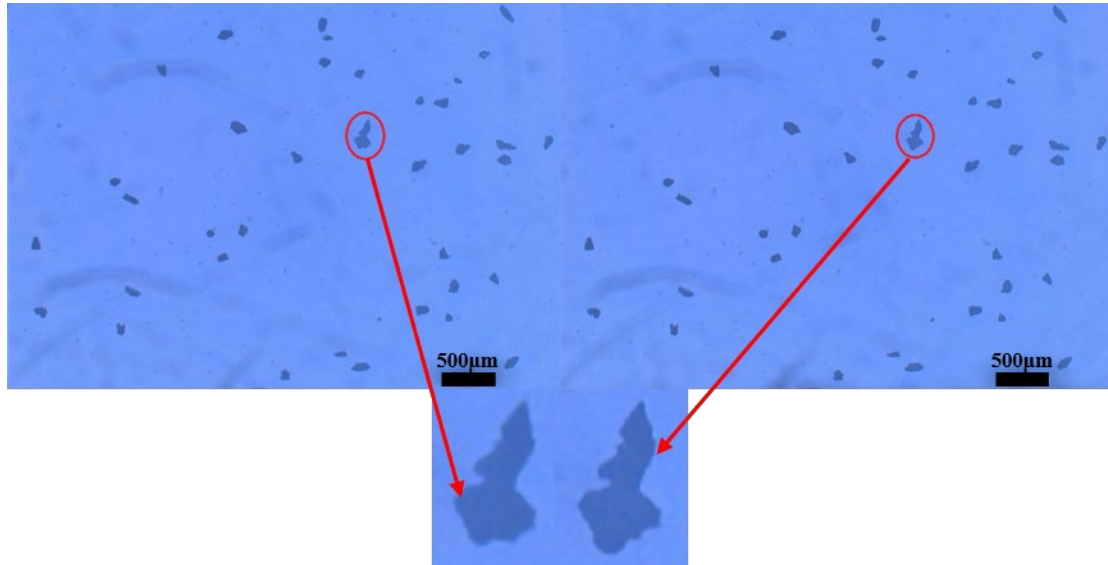
Fig. 12. Gas nucleation on graphite particle surfaces in oversaturated water without MIBC

3.4. Agglomeration experiments

MIBC does not show to influence the size distribution in tap water as presented in a previous study (Vanderbruggen et al., 2021). Fig. 13 shows the size distribution of the particles in the different conditions. Second modes appear between 100 μm - 500 μm in air-oversaturated water by aggregates formed. As shown in the results, the particles dispersed well with 2500 rpm of the magnetic stirrer in normal tap water without MIBC, so it means the formation of the second modes size distribution in air-oversaturated water with and without MIBC was due to the capillary bridging effect of the nucleation bubbles on graphites surface with this rotation speed (Paulson and Pugh, 1996). The experiments were repeated three times for each condition. The average proportion of particles and aggregates larger than 100 μm in air-oversaturated water with and without MIBC are 14.3 % ± 0.6 % and 17.0 % ± 1.0 %, respectively.
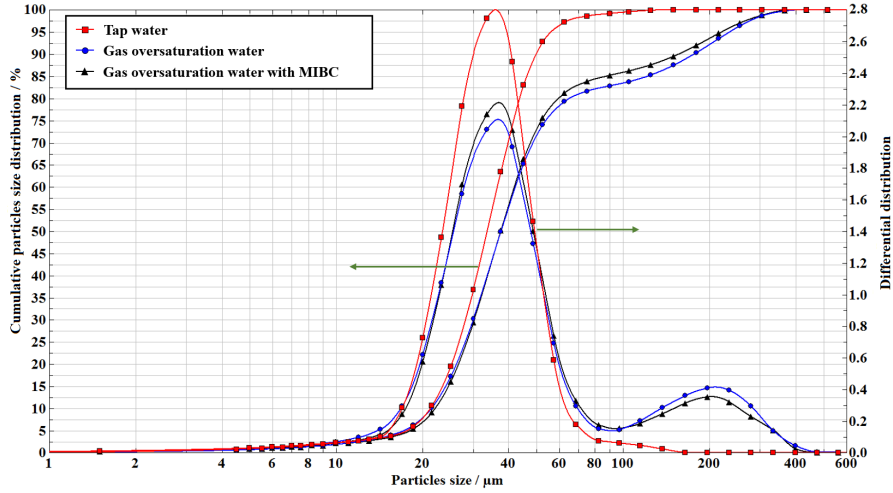
Fig. 13. The particle size distributions in air-oversaturated water with and without MIBC

4. Discussion

We define a critical height of the gas-liquid surface of a gas nucleus H to explain the influence of surface tension on the gas nucleation probability, as depicted in Fig. 14. At a certain degree of gas oversaturation, if the height of the gas-liquid surface is smaller than the critical height, the gas nucleus will dissolve and disappear, and if the height of the gas-liquid surface is larger than the critical height, the gas nucleus will be active to form a surface microbubble (Wilt, 1985; Zargarzadeh and Elliott, 2019).
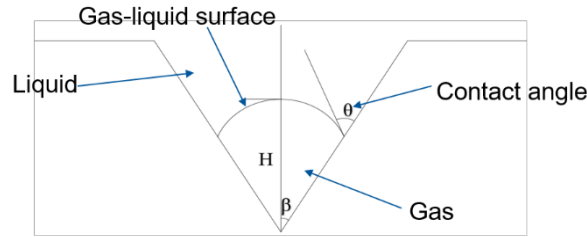

Fig. 14. the model of gas nuclei entrapped in a cove cavity

The contact angle θ will be influenced by the gas-liquid surface tension, the relationship between the contact angle and the gas-liquid surface tension is shown in the famous Young-Dupré equation (6)

$$cos\theta = \frac{\gamma_{SG} - \gamma_{SL}}{\gamma_{LG}} \quad (6)$$

where θ is the contact angle, γ_{LG} the surface tension of the gas-liquid surface, γ_{SG} the surface tension (or specific surface energy) of the solid-gas surface and γ_{SL} the interfacial tension of the

solid-liquid interface. After adding the surfactant, the contact angle in the solution will change, which is addressed in the following equations.

As shown in Fig. 14, a gas nucleus is entrapped in a cove cavity (the contact angle θ of the surface is 77° measured from the liquid phase and the half-angle β of the cove is 45°) under atmospheric pressure. The relationship between the height of the gas nucleus (H) and the radius of the gas-liquid meniscus (R) is shown in equation (7).

$$H = R\left[\frac{\cos(\theta-\beta)}{\tan\beta} + 1 - \sin(\theta - \beta)\right] \ (7)$$

The gas nucleus will grow when the gas concentration in the solution (c_∞) is bigger than the gas concentration (c_{LG}) on the gas-liquid surface of the gas nucleus. The degree of gas oversaturation (ζ) is expressed by equation (8).

$$\zeta = \frac{c_\infty}{c_s} \ (8)$$

Where c_s is the saturation concentration of air in water under certain temperature and pressure.

As shown in equations (9) and (10), c_{LG} is equal to Henry's constant (k_H) multiplied with the sum of gas pressure in the gas nucleus and laplace pressure of the gas liquid surface ($P_a + P_{LG}$).

$$P_{LG} = \frac{2\gamma_{LG}}{R} \ \ (9)$$

$$c_{LG} = k_H(P_a + P_{LG}) = k_H\left(P_a + \frac{2\gamma_{LG}}{R}\right) \ (10)$$

When the gas concentration in water (c_∞) is equal to the gas concentration (c_{LG}) on the gas-liquid surface of the gas nucleus under certain degree of gas oversaturation, the critical radius is given by the combination of eqs. (11), (12), (13), (14) and (15).

$$c_\infty = c_{LG} = k_H\left(P_a + \frac{2\gamma_{LG}}{R}\right) \ (11)$$

$$\frac{2\gamma_{LG}}{R} = \left(\frac{c_\infty}{k_H P_a} - 1\right)P_a \ (12)$$

$$c_s = k_H P_a \ (13)$$

$$\frac{2\gamma_{LG}}{R} = (\zeta - 1)P_a \ (14)$$

$$R = \frac{2\gamma_{LG}}{(\zeta-1)P_a} \ (15)$$

Combining eqs. (7) and (15), the critical height (H) can be obtained as equation (16):

$$H = \frac{2\gamma_{LG}}{(\zeta-1)P_a}\left[\frac{\cos(\theta-\beta)}{\tan\beta} + 1 - \sin(\theta - \beta)\right] \ (16)$$

From the measurements of surface tension using bubble pressure tensiometry at 20°C ($\pm$ 0.5°C),

the surface tension of the MIBC solution with a concentration of 1.5×10^{-5} mol/L is about 71.6 mN/m. Compared to the gas-liquid surface tension of normal tap water of 72.0 mN/m, the critical height (H) decreases by only about 0.4 %. However, the gas nucleation probability in this MIBC solution increased significantly. Thus, it seems that the decrease of the critical nucleation height caused by the reduction of surface tension is not the driving mechanism. The surfactant can adsorb on the gas-liquid surface to form a stable gas-liquid film which is benefitting the entrainment of gas nuclei into the solution. Many stable gas nuclei whose heights are larger than the critical height will be entrapped while the solid surfaces immerse in the MIBC solution, which can provide many gas nuclei for surface microbubble nucleation to improve the gas nucleation probability.

Bournival et al. (2014) found that MIBC can increase the damping coefficient of bubbles, namely, reduce the wave of bubble surfaces during the coalescence of bubble pairs, which can reduce the fraction of particles detached from bubble surfaces. When the MIBC concentration is bigger than 4×10^{-4} mol/L, the damping coefficient was found to increase, which they obtained by using the normalized relative projected area of coalescing bubble pairs (Bournival et al., 2014; Bournival et al., 2015; Bournival et al., 2012), which means the concentration of 1.5×10^{-5} mol/L MIBC in this study has minor effects on the damping coefficient. In this study, it can be found that 1.5×10^{-5} mol/L MIBC reduces the attachment of the particles in pick-up experiments and increases the particle-bubble load of the bubble in the bubble collision experiments which indicates low concentration MIBC can also reduce the fraction of particles detached. The discrepancy may be the different bubble oscillations in our study: it can be caused by the coalescence of bubbles but also by the wave of bubble surfaces induced by the hydrodynamic conditions. Aoki et al. (2015a, b) found that Taylor bubbles contaminated with 1-octanol and Triton X-100 rising through vertical pipes have immobile surfaces which can prevent the violent wave of bubble surfaces due to the Marangoni effect as compared to clean bubbles with mobile surfaces. It implies that the surfactant can weaken the wave in the bubble surfaces to reduce the detachment of particles. The slight shape oscillation of the immobile surfaces of carrying bubbles could be why such low concentration MIBC still has a significant influence on the detachment process. As the increase of the gas nucleation probability and the decrease of the detachment, MIBC can increase the load of particle-bubble aggregates and carrying bubbles to improve the recovery of graphite particles significantly.

5. Conclusion

In this study, the influences of gas nucleation by a frother-type surfactant MIBC on graphite flotation were investigated through micro-flotation, single bubble collision and pick-up experiments, microscopic observations, and agglomeration experiments. The flotation results show that the recovery of graphite increased by gas nucleation phenomena and the formation of aggregates in air-oversaturated water compared to normal tap water, and the effect of gas nucleation was further enhanced by MIBC. From the bubble collision and pick-up experiments, it can be found that MIBC can reduce the detachment of particles from the bubble surface to improve the coverage angle on the bubble surface significantly in hydrodynamic conditions. With the microscopic observations, the bubble nucleation processes have been recorded, and it can be seen that nucleation bubbles prefer to nucleate in the crevices and holes on the graphite surface. It can be observed that the floating aggregates were formed by the collision between nucleation micro-bubbles and graphite particles which can improve the recovery of fine particles. From the statistics of using gas nucleation probability, it can be found that MIBC can improve the gas nucleation probability in air-oversaturated water. From the agglomeration experiments, it can be observed that more coarser aggregates are formed in air-oversaturated water with MIBC compared to the case without MIBC. These results indicated that frother type surfactants have two critical influences on the flotation with air-oversaturated water: (1) improving the gas nucleation probability to form more surface microbubbles by enhancing the stability of surface nuclei; (2) increasing the particle load through the deacrease of particle detachment of carrying bubbles as well as aggregates which were composed of nucleation bubbles and graphite particles. There are many hydrophobic and rough minerals in the flotation industry that require a low degree of air-oversaturation in water for gas nucleation to occur. The frother-type surfactants are often used in flotation, which can improve the stability of surface nucleation bubbles besides its common use to decrease bubble size and impacting froth stability. In conclusion, this study highlights the importance of the combined effects of gas nucleation and frother action in flotation, especially for the recovery of fine particles.

References:

Alves, S.S., Orvalho, S.P., Vasconcelos, J.M.T., 2005. Effect of bubble contamination on rise velocity and mass transfer. Chem. Eng. Sci. 60(1), 1-9.

Aoki, J., Hayashi, K., Hosokawa, S., Tomiyama, A., 2015a. Effects of Surfactants on Mass Transfer from Single Carbon Dioxide Bubbles in Vertical Pipes. Chem. Eng. Technol. 38(11), 1955-1964.

Aoki, J., Hayashi, K., Tomiyama, A., 2015b. Mass transfer from single carbon dioxide bubbles in contaminated water in a vertical pipe. Int. J. Heat Mass Transfer 83, 652-658.

Aquilano, D., Costa, E., Genovese, A., Massaro, F.R., Rubbo, M., 2003. Heterogeneous nucleation and growth of crystalline micro-bubbles around gas cavities formed in solution. Prog. Cryst. Growth Charact. 46, 59-84.

Arturo, B.T., Roberto, P.G., Diego, M.C., 2015. Zeta potential of air bubbles conditioned with typical froth flotation reagents. Int. J. Miner. Process. 140, 50-57.

Bournival, G., Ata, S., Karakashev, S.I., Jameson, G.J., 2014. An investigation of bubble coalescence and post-rupture oscillation in non-ionic surfactant solutions using high-speed cinematography. J. Colloid Interface Sci. 414, 50-58.

Bournival, G., de Oliveira e Souza, L., Ata, S., Wanless, E.J., 2015. Effect of alcohol frothing agents on the coalescence of bubbles coated with hydrophobized silica particles. Chem. Eng. Sci. 131, 1-11.

Bournival, G., Pugh, R.J., Ata, S., 2012. Examination of NaCl and MIBC as bubble coalescence inhibitor in relation to froth flotation. Miner. Eng. 25(1), 47-53.

Cao, L., Chen, X.M., Peng, Y.J., 2021. The adsorption and orientation of frother surfactants on heterogeneous wetting surfaces. Appl. Surf. Sci. 548, 149225.

Chen, Y., Li, H., Feng, D., Tong, X., Hu, S., Yang, F., Wang, G., 2021. A recipe of surfactant for the flotation of fine cassiterite particles. Miner. Eng. 160.

Chipfunhu, D., Zanin, M., Grano, S., 2011. The dependency of the critical contact angle for flotation on particle size – Modelling the limits of fine particle flotation. Miner. Eng. 24(1), 50-57.

Chu, P., Mirnezami, M., Finch, J.A., 2014. Quantifying particle pick up at a pendant bubble: A study of non-hydrophobic particle–bubble interaction. Miner. Eng. 55, 162-164.

Farrokhpay, S., Filippova, I., Filippov, L., Picarra, A., Rulyov, N., Fornasiero, D., 2020. Flotation of fine particles in the presence of combined microbubbles and conventional bubbles, Miner. Eng. 155, 106439.

Hemmingsen, E.A., 1978. Effects of Surfactants and Electrolytes on the Nucleation of Bubbles in Gas-Supersaturated Solutions. Zeitschrift für Naturforschung A, 164-171.

Miettinen, T., Ralston, J., Fornasiero, D., 2010. The limits of fine particle flotation. Miner. Eng. 23(5), 420-437.

Jones, S.F., Evans, G.M., Galvin, K.P., 1999. Bubble nucleation from gas cavities-a review. Adv. Colloid Interface Sci. 80, 27-50.

Le, T.N., Phan, C.M., Nguyen, A.V., Ang, H.M., 2012. An unusual synergistic adsorption of MIBC and CTAB mixtures at the air–water interface. Miner. Eng. 39, 255-261.

Liu, A., Fan, P.P., Qiao, X.X., Li, Z.H., Wang, H.F., Fan, M.Q., 2020. Synergistic effect of mixed DDA/surfactants collectors on flotation of quartz. Miner. Eng. 159.

Liu, C., Ni, C., Yao, J., Chang, Z., Wang, Z., Zeng, G., Luo, X., Yang, L., Ren, Z., Shao, P., Duan, L., Liu, T., Xiao, M., 2021. Hydroxypropyl amine surfactant: A novel flotation collector for efficient separation of scheelite from calcite. Miner. Eng. 167.

Liu, J., Hu, Z., Liu, G., Huang, Y., Zhang, Z., 2019. Selective Flotation of copper oxide minerals with a Novel amino-triazole-thione surfactant: a comparison to hydroxamic acid collector. Miner. Process. Extr. Metall. Rev. 41(2), 96-106.

Miettinen, T., Ralston, J., Fornasiero, D., 2010. The limits of fine particle flotation. Miner. Eng. 23(5), 420-437.

Miller, J.D., Lin, C.L., Chang, S.S., 1983. MIBC adsorption at the coal/water interface. Colloids Surf. 7, 351-355.

Nguyen, A.V., Evans, G.M., 2004. Movement of fine particles on an air bubble surface studied using high-speed video microscopy. J. Colloid Interface Sci. 273, 271-277.

Nowak, E., Pacek, A.W., 2015. Method for the prediction of the particle attachment to the bubble in oil at elevated temperatures. Powder Technol. 274, 105-111.

Nuorivaara, T., Serna-Guerrero, R., 2020. Amphiphilic cellulose and surfactant mixtures as green frothers in mineral flotation. 1. Characterization of interfacial and foam stabilization properties. Colloids Surf., A 604, 125297.

Ozmak, M., Aktas, Z., 2006. Coal Froth Flotation Effects of Reagent Adsorption on the Froth structure. Energy Fuels 20, 1123-1130.

Paulson, O., Pugh, R.J., 1996. Flotation of Inherently Hydrophobic Particles in Aqueous Solutions of Inorganic Electrolytes. Langmuir 12 (20), 4808-4813.

Parhizkar, M., Edirisinghe, M., Stride, E., 2015. The effect of surfactant type and concentration on the size and stability of microbubbles produced in a capillary embedded T -junction device. RSC Adv. (14), 10751-10762.

Peng, W., Chang, L., Li, P., Han, G., Huang, Y., Cao, Y., 2019. An overview on the surfactants used in ion flotation. J. Mol. Liq. 286.

Pradhan, S., Qader, R.J., Sedai, B.R., Bikkina, P.K., 2019. Influence of wettability on pressure-driven bubble nucleation: A potential method for dissolved gas separation. Sep. Purif. Technol. 217, 31-39.

Ralston J., Fornasiero D., Hayes R., 1999. Bubble–particle attachment and detachment in flotation. Int. J. Miner. Process. 56, 133-164.

Ruan, Y., Deng, B., He, D., Chi, R., 2021. Synergetic effect of cottonseed fatty acid salt and nonionic surfactant NP-4 in the froth flotation of siliceous-calcareous phosphate rock. Colloids Surf., A 622.

Rulyov, N.N., Sadovskiy, D.Y., Rulyova, N.A., Filippov, L.O., 2021. Column flotation of fine glass beads enhanced by their prior heteroaggregation with microbubbles. Colloids Surf., A. 617.

Sabereh, N., Shafaei, S.Z., Mahdi, G., Rahman, A., Behzad, S., Fan M.M., 2019. Effects of nanobubble and hydrodynamic parameters on coarse quartz flotation. Int. J. Min. Sci. Technol. 29(2), 289-295.

Satpute, P.A., Earthman, J.C., 2021. Hydroxyl ion stabilization of bulk nanobubbles resulting from microbubble shrinkage. J. Colloid Interface Sci. 584, 449-455.

Shahbazi, B., Rezai, B., Javad Koleini, S.M., 2010. Bubble–particle collision and attachment probability on fine particles flotation, Chem. Eng. Process. 49(6), 622-627.

Tanaka, S., Kastens, S., Fujioka, S., Schlüter, M., Terasaka, K., 2020. Mass transfer from freely rising microbubbles in aqueous solutions of surfactant or salt. Chem. Eng. J. 387.

Vanderbruggen, A., Sygusch, J., Rudolph, M., Serna-Guerrero, R., 2021. A contribution to understanding the flotation behavior of lithium metal oxides and spheroidized graphite for lithium-ion battery recycling. Colloids Surf., A. 626, 127111.

Verrelli, D.I., Albijanic, B., 2015. A comparison of methods for measuring the induction time for bubble–particle attachment. Miner. Eng. 80, 8-13.

Wang, W.X., Zhou, Z.A., Nandakumar, K., Xu, Z.H., Masliyah, J.H., 2003. Attachment of individual particles to a stationary air bubble in model systems. Int. J. Miner. Process. 68(1-4), 47-69.

Wills B. A., Finch J. A., 2016. Chapter 12-Froth flotation. Wills' Mineral Processing Technology. 265-380.

Wilt, P.M., 1985. Nucleation rates and bubble stability in water-carbon dioxide solutions. J. Colloid Interface Sci. 122, 530-538.

Xiao, W., Zhao, Y.L., Yang, J., Ren, Y.X., Yang, W., Huang, X.T., 2019. Effect of sodium oleate on the adsorption morphology and mechanism of nanobubbles on the mica surface. Langmiur 35, 9239-9245.

Xu, M., Li, C.W., Wang, Y.T., Zhang H.J., 2019. Investigation on mechanism of intensifying coal fly ash froth flotation by pretreatment of non-ionic surfactant. Fuel 254.

Xu, M., Li, C.W., Zhang H.J., Kupka N., Peuker U.A., Rudolph M., 2022. A contribution to exploring the importance of surface air nucleation in froth flotation–The effects of dissolved air on graphite flotation. Colloids Surf., A. 633, 127866.

Yount, D.E., Gillary, E.W., Hoffman, D.C., 1984. A microscopic investigation of bubble formation nuclei. J. Acoust. Soc. Am. 76(5), 1511-1521.

Yuan, H., Tan, S., Feng, L., Liu, X., 2016. Heterogeneous bubble nucleation on heated surface from insoluble gas. Int. J. Heat Mass Transfer 101, 1185-1192.

Zargarzadeh, L., Elliott, J.A.W., 2019. Bubble formation in a finite cone: more pieces to the puzzle. Langmuir 35(40), 13216-13232.

Zhang, X., Uddin, M.H., Yang, H., Toikka, G., Ducker, W., Maeda, N., 2012. Effects of surfactants on the formation and the stability of interfacial nanobubbles. Langmuir 28(28), 10471-10477.

Zhao, W., Wei, S., Pingshan, W., Die, L., Haisheng, H., 2021. A novel metal–organic complex surfactant for high-efficiency mineral flotation. Chem. Eng. J. 426, 130853.